



¹⁸F-fluorodeoxyglucose PET/CT in aplastic anemia: a literature review and the potential of a computational approach

Practice points

- Bioptical diagnosis of aplastic anemia can be impractical, as bone marrow inhomogeneity frequently leads to inconclusive results.
- Positron emission tomography/computed tomography is a widely used imaging technique, allowing a whole body evaluation of the hematopoietic tissue, encompassing anatomical and functional information.
- ¹⁸F-fluorodeoxyglucose positron emission tomography/computed tomography is a feasible method to detect different stages of aplastic anemia: accordingly, different patterns of tracer distribution were detected in our series in patient studied in the active disease phase (autoimmune reaction), in the regenerative phase and the stable disease phase, respectively.

Aim: Aplastic anemia (AA) is a rare hematologic condition, characterized by bone marrow (BM) insufficiency, mostly on autoimmune basis. BM inhomogeneity hampers the diagnosis by bioptic sample. We propose a noninvasive evaluation of BM extension and metabolism in different AA stages. **Materials & methods:** Four AA patients (mean age: 45 ± 21 years, range: 18–63, 3 females) were submitted to whole-body ¹⁸F-fluorodeoxyglucose (FDG) positron emission tomography/computed tomography. We compared these patients with matched healthy controls, selected from a published normalcy database. **Results:** The presence of several hypermetabolic uptake areas was related to BM hypo/aplasia, while homogeneous, low grade FDG uptake was observed in patients in clinical remission. These data suggest that FDG positron emission tomography/computed tomography could be a noninvasive diagnostic complement in AA patients.

Keywords: aplastic anemia • bone marrow • FDG • hybrid imaging • PET/CT

Aplastic anemia (AA) is a rare nonmalignant hematologic condition, characterized by an incidence of two to four cases per million and a prevalence ranging from 19 to 48 per million, depending on the geographic area. It is a life-threatening disease [1], characterized by pancytopenia, reflecting the bone marrow (BM) inability to warrant self-renewal of residing hematopoietic stem cells and thus its capability to generate mature blood elements [2,3]. Accordingly, its diagnosis relies on biop-

tic finding of hematopoietic BM replacement by fat tissue.

Etiology still remains unclear, as exposure to toxins, use of certain drugs, a concomitant autoimmune disease, radiation exposure or genetic factors can all play a role in AA onset [1,2]. It is, however, unclear whether exposure to these factors is *per se* the cause of the disease or it merely acts as a trigger of a largely unknown process entailing an immune component whose role is confirmed by the effec-

Roberta Piva^{*1}, Francesco Fiz¹, Michele Piana², Francesca Bongioanni¹, Gianluca Bottoni¹, Andrea Bacigalupo³, Cecilia Marini⁴ & Gianmario Sambucetti¹

¹Nuclear medicine unit, Genoa University, IRCCS San Martino-IST, Genoa, Italy

²Department of Mathematics, University of Genoa, Genoa, Italy

³Department of hematology, Genoa University, IRCCS San Martino-IST, Genoa, Italy

⁴CNR Institute of Molecular Bioimaging & Physiology, Milan, Section of Genoa, Italy

*Author for correspondence:

Tel.: +39 010 555 4813

Fax: +39 010 555 6911

pivaroberta@hotmail.it

tiveness of immunosuppressive therapy in almost 70% of patients [3].

In these patients, imaging techniques played a relevant role in evaluating specific aspects of AA. In particular, X-ray computed tomography (CT) is often recommended to identify the possible occurrence of enlarged lymph nodes as possible sign of underlying lymphoma [4]. Similarly, this technique has been proposed to detect structural alterations in kidney and bones of arms and hands to ascertain or rule out Fanconi anemia [5]. However, imaging has been scarcely used to characterize BM failure as well as its underlying mechanism, its severity and its distribution. Indeed, even though biopsy offers an unsurpassed capability to characterize healthy and diseased hematopoietic function, the regional nature of sampling intrinsically implies to consider BM as a homogeneous organ. This assumption has been already challenged in patients with different types of lymphoma in whom biopsy failed in identifying foci of occult neoplastic disease, as these areas were far from the sampled site [6]. Moreover, in AA, several studies, based on ^{18}F -fluorodeoxyglucose (FDG) and on ^{18}F -fluorothymidine (FLT) positron emission tomography (PET) imaging, highlighted an exceedingly inhomogeneous BM metabolism [3,7–8]. However, this potential has never been evaluated in depth, while PET/CT imaging of FDG uptake has been most often used to define the effect of different treatments, including steroid hormones, chemotherapy and growth factors. In the AA setting, the application of growth factors actually highlighted areas of active BM spared by the disease [7,8].

Complementing the information derived by BM histopathology with a ‘bird’s-eye’ view of the entire hematopoietic organ might indeed improve our understanding of the so far elusive pathophysiology of this disease.

History of bone marrow imaging in aplastic anemia

In past decades, attempts of BM functional imaging were performed using radiolabeled compounds such as $^{99\text{m}}\text{Tc}$ -sulphur colloid, $^{99\text{m}}\text{Tc}$ -nanocolloid, ^{111}In -chloride and radiolabeled white blood cells as these substances can trace the reticuloendothelial system, the erythroid and myeloid compartments [3].

Nowadays, the progressive increase of PET imaging in the clinical routine improved our capability to characterize cellular metabolism and proliferative activity of BM by using tracers such as FDG and FLT [9]. Nevertheless, PET studies describing BM pattern in the aplastic patients are mainly case reports.

In 2005, Kouba *et al.* described the case of a 25-year-old woman with anemia and thrombocytopenia, sub-

mitted to trephine biopsy (revealing an aplastic marrow with cellularity less than 5%) and then treated with G-CSF [7]. A PET/CT scan was performed and revealed multiple focal lesions highly suspicious for disseminated localization of BM neoplastic disease. A subsequent PET/CT-directed-surgical biopsy was executed: hypercellular islands of healthy BM, mimicking malignancy, were found. This case highlights both the potential of PET/CT in guiding bioptic sampling of BM regions involved in disease process and the confounding effect of BM stimulating factors [7].

In 2009, an incidental finding on a pelvic scan provided the only magnetic resonance imaging (MRI) case report on BM aspect in AA. Image analysis showed a spotty T1 aspect of BM contained in sacral and lumbar vertebrae, as well as the one in the iliac wings and femura. Bioptic analysis confirmed reduced cellularity with areas of relative erythroid hyperplasia: the patient was then diagnosed as being affected by low-grade, asymptomatic AA [10].

In 2010, Cicone *et al.* reported a case of a 43-year-old man with severe pancytopenia whose BM biopsy revealed marked hypocellularity with no excess of blasts, megakaryocytes or fibrosis, associated with very rare erythroid and granulocytic precursors [8]. Afterward, the patient underwent conventional radiological imaging: vertebral areas with patchy hyperdensities were noticed at CT scan. At magnetic resonance, these areas expressed signal characteristics that were compatible with multiple neoplastic disease localization. Multiple myeloma diagnosis was excluded by searching for paraprotein with immunofixation of blood and urine and for serum-free light chains. To further investigate a possible tumoral origin of the patchy BM lesions, the patient was addressed to a FDG PET/CT scan that showed three vertebral foci of increased tracer uptake with respect to average BM standardized uptake value (SUV). To explain the clinical significance of this finding, biopsy was performed in a vertebral region with high tracer retention and provided the final diagnosis of nonpathologic, hyperplastic residual focus of hematopoiesis in a patient with AA.

So far, determinants of the increased FDG uptake of BM are still largely unknown: actually, glucose consumption is a basic aspect of all living cells. Accordingly, focal hot spots can represent both areas of active hematopoiesis and regions of inflammatory infiltration. Further investigations are needed in order to elucidate the possible association between FDG uptake and descriptors of hematologic conditions (including blood cells counts, previous chemo-/radiotherapy, hematopoietic stimulating factors).

Accordingly, correct evaluation of cellular metabolism cannot abide from a specific tracer. Fluoro-

deoxy-levo-thymidine is a pharmaceutical originally developed in the early-90s as nucleoside analog with antiretroviral activity [11]. Its ¹⁸F-radiolabelled analog (FLT) diffuses into the cell by a carrier-mediated mechanism, as well as by facilitated diffusion, and is phosphorylated to 3-fluorothymidine MP (FLT-MP) through the S-phase specific enzyme TK-1. This phosphorylation results in intracellular trapping of FLT-MP. Increased TK-1 activity is related to an increased rate of DNA synthesis, which is observed in rapidly growing cells as well as in many types of cancers [9]. FLT-PET might therefore be able to visualize the high cycling activity of hematopoietic cells in the BM compartment.

This tracer has been already exploited to evaluate AA patients testing the hypothesis that disease severity might actually be estimated by degree and distribution of tracer uptake in BM. In 2011, Agool *et al.* described 17 aplastic patients who underwent at least one FLT-PET scan and compared them with 11 nonhematological subjects [12]. The aplastic group was indeed heterogeneous: eight patients were studied at the time of the diagnosis, three at the time of relapse and six were in a condition of partial or complete remission. All patients underwent trephine biopsy and complete blood cell counts.

In the untreated group, Agool *et al.* noticed an increased uptake of FLT (with respect to the control patients) in some patchy areas of the vertebrae and a decreased SUV in the pelvic segment. On the other hand, a normal or increased pelvic tracer uptake and some 'hot spot' areas in the long bone shafts could be documented in three out of six patients in partial remission. Finally, complete remission was associated with a homogeneous tracer uptake throughout the whole skeleton, with no detectable hot spots and a regular distribution in the pelvic district.

On the basis of these data, the authors concluded that solitary areas of increased proliferative activity probably augment after treatment in patients with partial response: they might be responsible for the improvements in peripheral blood cell counts.

A volumetric approach to bone marrow imaging

The previously mentioned studies point out that imaging investigation of BM distribution can improve our capability to characterize AA highlighting presence and location of residual active BM. Specifically, advantages of imaging studies include the overall evaluation of the hematopoietic tissue and the nondependence from the sampling site. The information about BM extension and metabolism is virtually lacking as the only data about BM mass still rely on its first charac-

Table 1. Patients' characteristics.

Patient	Age	Hb	WBC	PLT	BM status	Axial BM PET aspect	Peripheral BM PET aspect	SUV mean	SUV max	Axial SUV deviation	Sacral SUV	Number of hotspots	Post PET recovery
V.A.	18	8.4	6.9	30	Hypoplastic with active flogosis	Homogeneously increased uptake	Diffuse spots	3.5 ± 4.2	21.4	3.4	9.1	28	Good
R.G.	63	9.3	1.9	7	Aplasia	Diffuse hypermetabolic spots	Rare spots	1 ± 1.1	9.8	1.2	2	11	Poor
S.A.	39	10.0	6.5	131	Mild hypoplasia with erythroid hyperplasia	Mostly homogeneous	Mostly homogeneous	0.8 ± 0.7	4.6	0.4	1.5	0	None, disease relapse
B.R.	60	8.8	1.1	16	Aplasia	Some hypermetabolic spots	Very rare spots	0.9 ± 0.8	14.2	0.9	1.9	8	Poor
Controls	60	N/A	N/A	N/A	Not assessed	Homogeneous	Homogeneous	0.9 ± 0.2	5.6	0.5	1.8	0	

BM: Bone marrow; Hb: Hemoglobin; PET: Positron emission tomography; PLT: Platelets; SUV: Standardized uptake value; WBC: White blood cells.

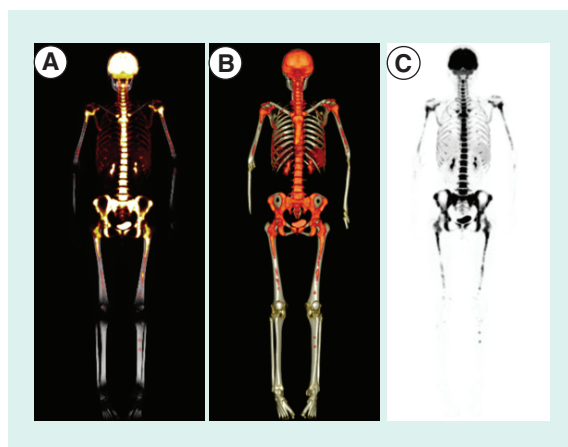


Figure 1. PET/CT maximum intensity projection of patient 1 shows a diffuse and homogeneous increase of FDG uptake in all vertebral bodies, in the pelvic region and in the proximal epiphysis of both humeral and femoral bones. Many focal areas of increased uptake of the tracer coexist in clavicular, ribs, scapulae and in femoral, tibial and fibular shafts. This patient presented hypocellular bone marrow with marked inflammatory infiltrate.
FDG: ^{18}F -fluorodeoxyglucose; PET/CT: Positron emission tomography/computed tomography

terization given by Mechanik in 1926 [13]. His experiment allowed a surprisingly precise evaluation of the total BM volume in 'normal subjects' and these data are still the standard for the dosimetry calculation in the setting of radiation therapy [14–16].

Definition of BM parameters with a noninvasive imaging approach could be hampered by several limitations. In fact, although the potential of MRI in evaluating BM composition [17–19] is well recognized, as T1 signal intensity can be used to discriminate active from inactive BM [20], the complexity of acquisition procedure and the influence of signal distortion artifacts limited its use to specific bone districts.

On the other hand, although modern-day CT algorithms significantly reduced radiation burden, total body application of this technique still implies an important radiation exposure [21].

In the effort to provide a sensitive and noninvasive method to study BM parameters, our group developed a software program, which is applied to hybrid PET/CT images, able to perform a computational integration of anatomical and functional information of the entire BM [22]. This approach has the advantage of studying the entire patient in a single scan, encompassing both volumetric and metabolic information, from CT and PET data, respectively. In the specific AA setting, the volumetric approach allows a precise definition of the space where the hematopoietic tissue is housed, which can be used to derive metabolic BM parameters.

Study aim

In the present study, we aim to summarize the attempts executed so far in characterizing BM behavior in AA and to propose a criterion for visual assessment of FDG PET/CT images in the AA patient. We also aim to ascertain whether to any given bioptic picture (normal BM vs hypoplasia vs aplasia) corresponds a definite FDG distribution pattern.

We will furthermore apply a computational method to the PET/CT images, as to complement the qualitative characterization of glucose BM metabolism in AA with quantitative data on its metabolism.

Materials & methods

Patient population

Our study included four patients (mean age 45 ± 21 , range 18–63) with AA. As shown in Table 1, the group included one man and three women, all of them in course of treatment (testosterone undecanoate and cyclosporine A). Patients were submitted to whole-body FDG PET/CT imaging to metabolically characterize different findings, recognized on a recent CT scan. According to our standard procedure, all patients signed a written informed consent form, encompassing the use of anonymized data for research purpose, before PET/CT examination.

We compared these patients with matched healthy controls, randomly selected from a published normalcy database [22]. Briefly, this database includes patients submitted to PET/CT scan as a long-term control of completely excised first-stage melanoma, never submitted to any chemo- or radiotherapy and negative at a 2-year follow-up.

PET-CT acquisition & reconstruction

After a minimum of 12-h fasting, serum glucose was assessed to ensure glucose level ≤ 1 g/l. Weight and height of all patients were measured. A bolus injection of FDG was then performed (4.8–5.2 MBq per kilogram of body weight) while patients were lying in supine position in a quiet room and instructed not to move or talk. PET imaging started 60–75 min after tracer administration and was performed in 3D mode, using an integrated PET/CT scanner (Hirez; Siemens Medical Solutions, TN, USA). The whole body was scanned from vertex to toes in an 'arms down' position. PET raw data were reconstructed by means of ordered subset expectation maximization (3 iterations, 16 subsets) and attenuation correction was performed using CT data. The transaxial field of view and pixel size of the reconstructed PET images were 58.5 cm and 4.57 mm, respectively, with a matrix size of 128×128 . As per standard PET/CT imaging protocol, 16-detector row helical CT scan was performed

with nondiagnostic current and voltage settings, with a gantry rotation speed of 0.5 s and table speed of 24 mm per gantry rotation. No contrast medium was injected. The entire CT dataset was fused with the 3D PET images using an integrated software interface (Syngo; Siemens Erlangen, Germany).

Image analysis: a computational approach

Image analysis was performed according to the previously validated method [22]. The algorithm identifies the skeleton on CT images by assuming that compact bone is the structure with the highest X-ray attenuation coefficient in the human body. Once identified the skeletal border, the program starts the thresholding algorithm, which samples a two-voxel-thick layer and computes its average Hounsfield value. Thereafter, all skeletal voxels having attenuation coefficient equal or above this value are considered as compact bone, the remaining trabecular bone. The software output is the extraction and 3D representation of three different volumes: skeletal volume, compact bone volume and trabecular bone volume. Then, two nuclear physicians (with 5 years' experience in PET/CT images reporting) manually proceeded to exclude the spinal cord and the nonskeletal calcified regions.

Trabecular bone volume is then voxel-wise multiplied against the PET co-registered data to extract and represent BM metabolic activity. The skull is intentionally excluded from the analysis, since brain radioactivity spillover prevents an accurate assessment of BM FDG uptake in this region. The computation of whole skeletal volumes was completed by a further segmental analysis: vertebrae and sternum accounted for the axial skeleton; humeral, femoral and tibial/fibular shafts for the appendicular skeleton.

All volumetric data were normalized for ideal body weight. All trabecular bone volume voxels were subdivided into active or inactive BM according to previously published statistical standards [22]. This criterion assumes that lumbar and thoracic vertebrae are almost fully occupied by active BM. In this district, average SUV was found to be 2.01 ± 0.36 in a population of 102 normal subjects. Assuming a normal distribution of these values, values of SUV located 2.5 standard deviations (SDs) below the average (i.e., < 1.11) were considered as idle, fatty BM. Active BM was defined as all intraosseous voxels, in all skeletal segments, with FDG uptake > 1.11 .

SUV_{mean} was defined as the average value of SUV of all intraosseous voxels, while SUV_{max} was defined as the value of the single voxel with the highest SUV; the former parameter was calculated both in the whole trabecular volume and in the active BM.

Average axial SUV was computed as the mean of all voxel belonging to the trabecular bone section within the spine and the sternum. On these segments, we also recorded average SD of SUV. Segmentation was then focused on the hips and sacrum, as to calculate the average metabolic activity of these skeletal segments. Liver metabolism was used as a standard of reference to normalize the medullary values and was defined using a 15-cm-wide region of interest, placed on the right hepatic lobe, from which the average glucose uptake index was obtained.

Results

Clinical findings

At the moment of PET/CT, the four aplastic patients were all in course of treatment but in different stages of the disease, with peculiar characteristics in blood cell counts and in BM cellularity (Table 1).

The first patient was transfusion-dependent with normal hemoglobin and leucocyte levels, moderate thrombocytopenia and a BM biopsy characterized by a three-line hypoplasia and findings suggestive for active inflammation.

The second patient was also transfusion-dependent, with normal blood cell counts and a very important thrombocytopenia. His BM was completely aplastic at the biopsy.

By contrast, the third patient had evidence of normalcy at the blood cell count and mild hypoplasia with only erythroid hyperplasia at the BM biopsy.

Last, the fourth patient showed very low leucocytes and platelet levels, in a context of an acellular mar-

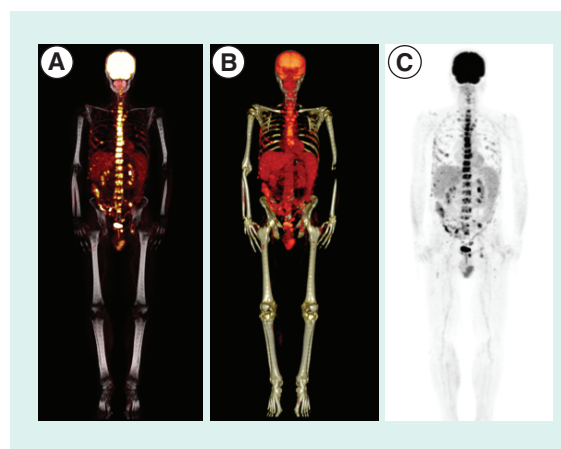


Figure 2. PET/CT scan of patient 2 describes the presence of many hypermetabolic spots in all the vertebrae, clavicae, costae and in the pelvic district; rare foci of increased FDG uptake were observed in the very proximal diaphysis of both femurs. Bone marrow biopsy showed a picture of complete aplasia. FDG: ¹⁸F-fluorodeoxyglucose; PET/CT: Positron emission tomography/computed tomography.

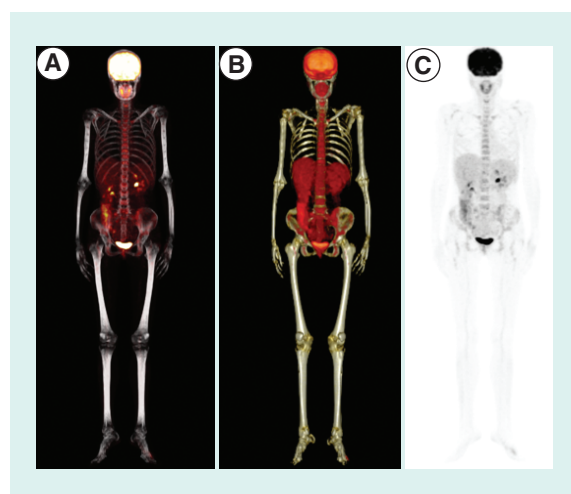


Figure 3. PET/CT images of patient 3 document a normal, homogenous and low-grade tracer uptake in both axial and appendicular skeleton. Bone marrow was mildly hypoplastic, but erythroid line was expanded.
PET/CT: Positron emission tomography/computed tomography.

row. Patients' clinical features are summarized in Table 1.

Image analysis: metabolic findings

Qualitative analysis of the 3D representation of the hybrid images showed a significant variability between patients.

The first patient was characterized by a homogeneously increased FDG uptake, which was, in the axial skeleton, roughly five-times higher than the control population. Many focal areas of increased uptake of the tracer coexisted in long bone's epiphysis and in the shafts of femura, tibiae and fibulae (Figure 1).

Images of the second patient showed diffuse hypermetabolic spots in all the vertebrae, costae and in the pelvic district; rare foci of increased FDG uptake were observed in the proximal diaphysis of both femurs (Figure 2).

A normal, homogenous and low-grade tracer uptake was documented in both axial and appendicular skeleton of the third patient (Figure 3).

However, some hypermetabolic spots were noticed in axial and peripheral skeleton of the fourth patient (Figure 4).

Image analysis: computational data

Subsequently, computational analysis of the entire skeleton allowed the extraction of several functional parameters from the automatically segmented BM. Table 1 lists all the major computational findings.

Patient 1 presented an overall increase of BM metabolism ($SUV_{mean} 3.5 \pm 4.2$): this increase was par-

ticularly marked in the hipbones. An exceptionally high SUV_{max} and a very pronounced inter-voxel variability accounted for the 'spotty' distribution of the tracer (Figure 1).

Patient 2 presented a similar, yet somewhat diminished, FDG-distribution pattern with respect to the first patient. His SUV_{mean} and the sacral mean metabolic index were only modestly increased when compared with the control population; the axial SUV_{SD} and SUV_{max} were coherent with the patchy aspect of this BM district (Figure 2).

The third patient showed BM computational parameters that were substantially similar to the control populations' ones (Figure 3).

Finally, the fourth patient presented a generally normal SUV_{mean} despite of an increase in SUV_{max} and SD , which were due to the presence of several hotspots (Figure 4).

Discussion

Role of FDG in AA assessment

To this day, attempts of *in vivo* radionuclide characterization of AA have been scarce. It is somehow paradoxical how the number of studies using a tracer of cellular proliferation – FLT – exceeds the ones using the most common PET imaging radiopharmaceutical, that is, FDG [3,7–8,22]. The reason behind this choice is probably the lack of specificity of the glucose analog, which traces both disease-related autoimmune process and BM proliferative response. By contrast, the FLT specificity for cells that are in the S phase of the cell cycle allows the reader to focus on the identification of areas of compensatory proliferation, which are essential as to ensure a good outcome [11]. It has to be noted that thymidine uptake could be seen even in areas of proliferating lymphocytes, whereas an autoimmune reaction is occurring. However, FDG would trace overall glucose consumption, whether related to proliferation or to the inflammatory pathways activation, whilst FLT uptake in inflammatory lesions is very low [23].

In spite of the low specificity, FDG foci observed in PET scans have been bioptically characterized as areas of healthy BM proliferation [7,8]. Conversely, a pattern of decreased metabolism, which was a common finding in the FLT series by Agool, was never paralleled by FDG in our group [12]. Our data suggest indeed that an increased metabolism, either diffuse (Figure 1) or spotty (Figures 2 & 4), indicated a condition of BM damage, which is correlated with worse platelet counts and a need for repeated transfusions. In opposition, a homogenous and low-grade FDG uptake, with average SUV comparable to those observed in the control cohort, was observed in the patient with normal cell counts (Figure 3).

Models of tracer distribution in different AA stages

Overall, these data suggest a possible clinical role for FDG PET in AA evaluation. In spite of the difficult interpretation of the diverse process underlying this disease, there are some common findings worth mentioning, which could enable the clinician to assess the global status of the hematopoietic tissue. In fact, imaging presentation of this disease could be narrowed down to two main scenarios, based on the characteristics of tracer distribution within the BM.

The first one represents the stage of the ongoing, active disease (Figures 2 & 4). In this case, the patient is generally pancytopenic, with abnormal findings at BM biopsy (hypo- or acellular BM). At PET/CT examination the uptake is spotty, showing some to several high-uptake areas, distributed throughout the axial (and in some cases even into the peripheral) BM. In the axial skeleton, SUV_{max} and SD of voxel SUV within the BM are extremely high, testifying the presence of hypermetabolic foci.

These ‘hot spots’ probably represent areas of hematopoietic tissue that have been spared by the autoimmune process and are thus hypermetabolic in order to compensate for the remaining hypocellular marrow; their uptake can be further increased with BM stimulant cytokines. Even if the ‘patchy’ aspect of FDG distribution correlates with a phase of active disease, the presence of marked hypermetabolism within these foci seems to bode well for the patients’ hematologic recovery.

In the second scenario, we have a homogenous tracer distribution within the whole intraosseous space, where the physiologic axial-appendicular metabolic gradient is respected and the areas of increased uptake are rare to none (Figure 3). This represents the stage of full BM recovery, with satisfactory cell counts and normal findings at the BM biopsy. This picture does not rule out the presence of latent disease nor can exclude future relapses; it does, however, reassure the clinician on the presence of a healthy and normally distributed BM and could be used, along with clinical and pathological parameters, to modulate the immunosuppressant therapy.

There is also a third possible scenario, which is represented by the overall hyperactivation of the whole BM (Figure 1). In this case, a bioptic evidence of inflammatory infiltrate paralleled the radiologic aspect. This picture is probably of rare occurrence; as to witness such an imaging scenario, PET scan should be performed during the time of the acute autoimmune reaction. For this reason, it is unlikely that such findings could be of help in establishing a definite diagnosis of active disease.

In opposition, the presence of foci of increased activity seems to be a hallmark of this disease. While the spotty FDG distribution in the trabecular bone signals a condition of BM distress, the presence of these spots is, however, key to a successful recovery. As of today, further studies are needed, to better elucidate the role of the radioisotopic evaluation of this disease. The present study however highlights a good sensitivity of the FDG PET/CT modality in the characterization of BM behavior in the course of this ailment.

Conclusion & future perspective

The multimodal nature of PET/CT scans and the high sensitivity of FDG uptake have indeed been successfully applied to different hematological disorders, such as myelofibrosis [24], documenting a generalized increase in glucose metabolism in BM together with high tracer uptake in enlarged spleen and liver. Although clinical experience reported in the literature in this setting is extremely limited, these and our results pave the way for multimodal imaging in future studies, encompassing larger populations, aiming to characterize BM response in different hematologic conditions.

In this line, the evidence of a heterogeneous distribution of glucose metabolism throughout the BM [25] confirms the potential of PET/CT imaging as a toll to identify skeletal segments target for biopsy sampling.

Indeed, an approach making use of pattern recognition algorithms, based on scoring system, such as the one proposed by Agool [25], can be of help in establishing a clinical threshold. In our series, we observed that SUV SD was a fitting parameter in describing

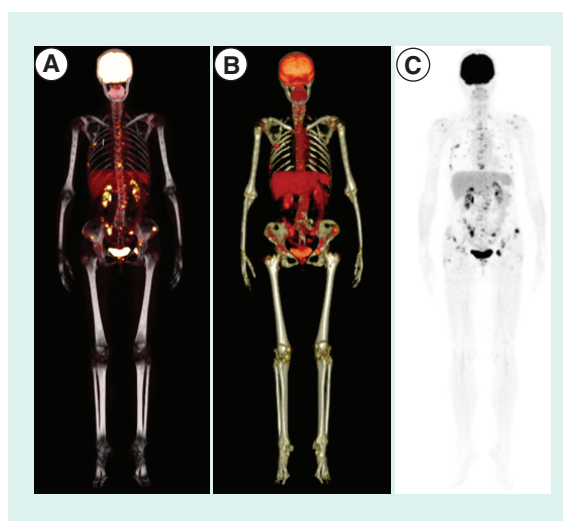


Figure 4. Some hypermetabolic spots are noticeable in vertebral bodies, ribs, hips and femoral proximal epiphysis of fourth patient's PET/CT scan. Similar to patient 2, the bone marrow of this patient was acellular. PET/CT: Positron emission tomography/computed tomography.

disease aggressiveness; this finding must however be standardized and confirmed in larger studies.

The application of the hybrid radiological and radio-isotopic technique will allow a better understanding of the nature and mechanisms of AA and potentially of other BM affections, enabling the clinician to perform a prognostic assessment and to perform a tailored treatment, based on the synergic evaluation of clinical, hematological, bioptical and imaging data. Development and diffusion of the next generation of PET/CT scanners, encompassing higher spatial resolution and less sensitive to noise, will enable the imaging specialist to further improve our understanding on the meta-

bolic pattern of this condition. This evidence-based approach could improve the efficacy of the existing therapies and the overall quality of life.

Financial & competing interests disclosure

The authors have no relevant affiliations or financial involvement with any organization or entity with a financial interest in or financial conflict with the subject matter or materials discussed in the manuscript. This includes employment, consultancies, honoraria, stock ownership or options, expert testimony, grants or patents received or pending, or royalties.

No writing assistance was utilized in the production of this manuscript.

References

Papers of special note have been highlighted as:

• of interest; •• of considerable interest

- 1 Young NS. Acquired aplastic anemia. *Ann. Intern. Med.* 136, 534–546 (2002).
- 2 Young NS, Calado RT, Scheinberg P. Current concepts in the pathophysiology and treatment of aplastic anemia. *Blood* 108, 2509–2519 (2006).
- 3 Agool A, Glaudemans AW, Boersma HH, Dierckx RA, Vellenga E, Slart RH. Radionuclide imaging of bone marrow disorders. *Eur. J. Nucl. Med. Mol. Imaging* 38, 166–178 (2011).
- 4 Suzuki Y, Niitsu N, Hayama M et al. Lymphoproliferative disorders after immunosuppressive therapy for aplastic anemia: a case report and literature review. *Acta Hematol.* 121, 21–26 (2009).
- 5 Demaerel P, Kendall BE, Kingsley D. Cranial CT and MRI in diseases with DNA repair defects. *Neuroradiology* 34, 117–121 (1992).
- 6 Moog F, Bangerter M, Kotzerke J, Gohlmann A, Frickhofen N, Reske SN. ¹⁸F-FDG PET as a new approach to detect lymphomatous bone marrow. *J. Clin. Oncol.* 16, 603–609 (1998).
- 7 Kouba M, Maaloufova J, Campr V, Belohlavek O, Drugova B. G-CSF stimulated islands of hematopoiesis mimicking disseminated malignancy on PET-CT and MRI scans in a patient with hypoplastic marrow disorder. *Br. J. Hematol.* 130, 807 (2005).
- A case-report on the proliferative nature of increased ¹⁸F-FDG-uptake bone marrow areas.
- 8 Cicone F, Stalder M, Geiger D, Cairoli A, Delaloye AB, Prior JO. Visual and quantitative approach to bone marrow foci of increased glucose uptake on PET/CT in a case of aplastic anemia. *Nuklearmedizin* 49(2), N10–2 (2010).
- A case report on the proliferative nature of the FDG-avid hot spots in AA.
- 9 Wagner M, Seitz U, Buck A et al. 3'-[¹⁸F]fluoro-3'-deoxythymidine ([¹⁸F]-FLT) as positron emission tomography tracer for imaging proliferation in a murine B-cell lymphoma model and in the human disease. *Cancer Res.* 63, 2681–2687 (2003).
- 10 De Mola RL, Kurre P. MRI findings in aplastic anemia. *Am. J. Hematol.* 84(11), 754 (2009).
- 11 Kong X, Zhu Q, Vidal P et al. Comparisons of anti-human immunodeficiency virus activities, cellular transport, and plasma and intracellular pharmacokinetics of 3-fluoro-3-deoxythymidine and 3-azido-3-deoxythymidine. *Antimicrob. Agents Chemother.* 36, 808–818 (1992).
- 12 Agool A1, Slart RH, Kluin PM, de Wolf JT, Dierckx RA, Vellenga E. ¹⁸F-FLT PET: a noninvasive diagnostic tool for visualization of the bone marrow compartment in patients with aplastic anemia: a pilot study. *Clin. Nucl. Med.* 36(4), 286–289 (2011).
- Represents a relevant nuclear medicine-based insight in AA pathophysiology, employing a relatively large patients' population.
- 13 Mechanik N. Untersuchungen ueber das Gewicht des knochenmarck des Menschen. *Zeitschripte fur gesamte anatomie* (79(1-2), 58–99 (1926).
- The forebear of attempts of bone marrow volume quantification in the human beings.
- 14 Atkinson HR. Bone marrow distribution as a factor in estimating radiation to the blood forming organs: a survey of present knowledge. *J. Coll. Radiol. Australas.* 6, 149–154 (1962).
- 15 Ellis RE. The distribution of active bone marrow in the adult. *Phys. Med. Biol.* 26, 389–400 (1981).
- 16 Woodard HQ, Holodny E. A summary of the data of Mechanik on the distribution of human bone marrow. *Phys. Med. Biol.* 5, 57–59 (1960).
- 17 Duda SH, Laniado M, Schick F et al. Normal bone marrow in the sacrum of young adults: differences between the sexes seen on chemical-shift MR imaging. *Am. J. Roentgenol.* 164, 935–940 (1995).
- 18 Kugel H, Jung C, Schulte O et al. Age- and sex-specific differences in the 1H-spectrum of vertebral bone marrow. *J. Magn. Reson. Imaging* 13, 263–268 (2001).
- 19 Basu S, Houseni M, Bural G et al. Magnetic resonance imaging based bone marrow segmentation for quantitative calculation of pure red marrow metabolism using 2-Deoxy-2-[F-18]fluoro-D-glucose-positron emission tomography: a novel application with significant implications for combined structure-function approach. *Mol. Imaging Biol.* 9, 361–365 (2007).

- 20 Vande Berg BC, Malghem J, Lecouvet FE *et al.* Magnetic resonance imaging of normal bone marrow. *Eur. Radiol.* 8, 1327–1334 (1998).
- 21 Romagnoli A, Funel V, Mechini A *et al.* Optimisation of low dose CT with adaptive statistical iterative reconstruction in total body examination. *Radiol. Med.* 117, 1333–1346 (2012).
- 22 Sambuceti G, Brignone M, Marini C *et al.* Estimating the whole bone-marrow asset in humans by a computational approach to integrated PET/CT imaging. *Eur. J. Nucl. Med. Mol. Imaging.* 39, 1326–1338 (2012).
- Normalcy database for extension and distribution of active and inactive bone marrow in healthy subjects.
- 23 Lee TS, Ahn SH, Moon BS *et al.* Comparison of ¹⁸F-FDG, ¹⁸F-FET and ¹⁸F-FLT for differentiation between tumor and inflammation in rats. *Nucl. Med. Biol.* 36, 681–686 (2009).
- Role of FLT/FDG positron emission tomography in distinguishing tumor and flogosis.
- 24 Khanna V, Nama S, Tailor R, Muthukrishnan A. Myelofibrosis on ¹⁸F-FDG-PET/CT in a case suspicious for post-transplant lymphoproliferative disorder. *Hell. J. Nucl. Med.* 12, 274–275 (2009).
- 25 Agool A, Schot BW, Jager PL, Vellenga E. ¹⁸F-FLT PET in hematologic disorders: a novel technique to analyze the bone marrow *J. Nucl. Med.* 47, 1592–1598 (2006).
- A representation of bone marrow proliferative asset in several hematologic disorders.